



HAL
open science

Adult Low-Hypodiploid Acute Lymphoblastic Leukemia Emerges from Preleukemic TP53 -Mutant Clonal Hematopoiesis

Rathana Kim, Hugo Bergugnat, Lise Larcher, Matthieu Duchmann, Marie Passet, Stéphanie Gachet, Wendy Cuccuini, Marina Lafage-Pochitaloff, Cédric Pastoret, Nathalie Grardel, et al.

► **To cite this version:**

Rathana Kim, Hugo Bergugnat, Lise Larcher, Matthieu Duchmann, Marie Passet, et al.. Adult Low-Hypodiploid Acute Lymphoblastic Leukemia Emerges from Preleukemic TP53 -Mutant Clonal Hematopoiesis. *Blood Cancer Discovery*, 2023, 4 (2), pp.134-149. 10.1158/2643-3230.BCD-22-0154 . hal-04090842

HAL Id: hal-04090842

<https://u-paris.hal.science/hal-04090842v1>

Submitted on 26 Sep 2023

HAL is a multi-disciplinary open access archive for the deposit and dissemination of scientific research documents, whether they are published or not. The documents may come from teaching and research institutions in France or abroad, or from public or private research centers.

L'archive ouverte pluridisciplinaire **HAL**, est destinée au dépôt et à la diffusion de documents scientifiques de niveau recherche, publiés ou non, émanant des établissements d'enseignement et de recherche français ou étrangers, des laboratoires publics ou privés.

Adult Low-Hypodiploid Acute Lymphoblastic Leukemia Emerges from Preleukemic *TP53*-Mutant Clonal Hematopoiesis

Rathana Kim^{1,2}, Hugo Bergugnat², Lise Larcher^{1,2}, Matthieu Duchmann¹, Marie Passet^{1,2}, Stéphanie Gachet¹, Wendy Cuccuini^{2,3}, Marina Lafage-Pochitaloff^{3,4}, Cédric Pastoret⁵, Nathalie Grardel⁶, Vahid Asnafi⁷, Beat W. Schäfer⁸, Eric Delabesse⁹, Raphaël Itzykson^{1,10}, Lionel Adès^{1,10}, Yosr Hicheri¹¹, Yves Chalandon¹², Carlos Graux¹³, Patrice Chevallier¹⁴, Mathilde Hunault¹⁵, Thibaut Leguay¹⁶, Françoise Hugué⁹, Véronique Lhéritier¹⁷, Hervé Dombret¹⁰, Jean Soulier^{1,2}, Philippe Rousset¹⁸, Nicolas Boissel¹⁰, and Emmanuelle Clappier^{1,2}

ABSTRACT

Low hypodiploidy defines a rare subtype of B-cell acute lymphoblastic leukemia (B-ALL) with a dismal outcome. To investigate the genomic basis of low-hypodiploid ALL (LH-ALL) in adults, we analyzed copy-number aberrations, loss of heterozygosity, mutations, and cytogenetics data in a prospective cohort of Philadelphia (Ph)-negative B-ALL patients ($n = 591$, ages 18–84 years), allowing us to identify 80 LH-ALL cases (14%). Genomic analysis was critical for evidencing low hypodiploidy in many cases missed by cytogenetics. The proportion of LH-ALL within Ph-negative B-ALL dramatically increased with age, from 3% in the youngest patients (under 40 years old) to 32% in the oldest (over 55 years old). Somatic *TP53* biallelic inactivation was the hallmark of adult LH-ALL, present in virtually all cases (98%). Strikingly, we detected *TP53* mutations in posttreatment remission samples in 34% of patients. Single-cell proteogenomics of diagnosis and remission bone marrow samples evidenced a preleukemic, multilineage, *TP53*-mutant clone, reminiscent of age-related clonal hematopoiesis.

SIGNIFICANCE: We show that low-hypodiploid ALL is a frequent entity within B-ALL in older adults, relying on somatic *TP53* biallelic alteration. Our study unveils a link between aging and low-hypodiploid ALL, with *TP53*-mutant clonal hematopoiesis representing a preleukemic reservoir that can give rise to aneuploidy and B-ALL.

See related commentary by Ogawa and Saiki.

¹Université Paris Cité, Institut de Recherche Saint-Louis (IRSL), Institut National de la Santé et de la Recherche Médicale (INSERM) U944, Centre National de la Recherche Scientifique (CNRS) UMR 7212 GenCellDis, Paris, France. ²Laboratoire d'Hématologie, Hôpital Saint-Louis, Assistance Publique-Hôpitaux de Paris (AP-HP), Paris, France. ³Groupe Francophone de Cytogénétique Hématologique (GFCH), Paris, France. ⁴Laboratoire de Cytogénétique Hématologique, Hôpital Timone Enfant, AP-HM, Aix-Marseille Université, Marseille, France. ⁵Laboratoire d'Hématologie, Centre Hospitalier Universitaire de Rennes, Rennes, France. ⁶Laboratoire d'Hématologie, Centre Hospitalier Régional Universitaire de Lille, Lille, France. ⁷Laboratoire d'Onco-hématologie, Hôpital Necker Enfants-Malades, AP-HP, Paris, France. ⁸Department of Hematology, University Hospital, Zürich, Switzerland. ⁹Institut Universitaire du Cancer de Toulouse-Oncopole, Toulouse, France. ¹⁰Département d'Hématologie Clinique, Hôpital Saint-Louis, AP-HP, Institut de Recherche Saint-Louis, Université Paris Cité, Paris, France. ¹¹Hematology Department, Institut Paoli-Calmettes, Aix Marseille Univ, CNRS, INSERM, CRCM, Marseille, France. ¹²Hématologie, Hôpitaux Universitaires de Genève, Genève, Switzerland. ¹³Université Catholique de Louvain, Centre Hospitalier

Universitaire UCLouvain Namur-Godinne, Service d'Hématologie, Yvoir, Belgium. ¹⁴Department of Hematology, CHU Nantes, INSERM UMR1232 and CNRS ERL6001 CRCINA IRS-UN, Nantes, France. ¹⁵Département des Maladies du sang, CHU Angers, FHU GOAL, Université d'Angers, Université de Nantes, INSERM, CNRS, CRCI2NA, SFR ICAT, Angers, France. ¹⁶Department of Hematology, CHU de Bordeaux, Hôpital du Haut-Levêque, Pessac, France. ¹⁷Coordination du Groupe GRAALL, HCL, Hôpital Lyon Sud, Lyon, France. ¹⁸Hematology Department, Centre Hospitalier de Versailles, UMR 1184 CEA, University Paris-Saclay, Le Chesnay, France.

Corresponding Author: Emmanuelle Clappier, Laboratoire d'Hématologie, Hôpital Saint-Louis, 1 Avenue Claude Vellefaux, 75010 Paris, France. Phone: 33-1-53-72-68-10; E-mail: emmanuelle.clappier@aphp.fr

Blood Cancer Discov 2023;4:1–16

doi: 10.1158/2643-3230.BCD-22-0154

This open access article is distributed under the Creative Commons Attribution-NonCommercial-NoDerivatives 4.0 International (CC BY-NC-ND 4.0) license.

©2023 The Authors; Published by the American Association for Cancer Research



Downloaded from <https://ascipublishing.org/bloodcancerdiscovery/article-pdf/doi/10.1159/2643-3230.BCD-22-0154/3269427/bcd-22-0154.pdf> by guest on 26 September 2023

26 INTRODUCTION

27 B-cell precursor acute lymphoblastic leukemia (B-ALL) repre-
28 sents a rare malignancy in adults associated with a poor prog-
29 nosis, especially in the older range of patients (1-3). Despite
30 significant improvements provided by pediatric-inspired treat-
31 ment regimens (4), there is still an important discrepancy
32 between B-ALL outcomes in children and adults, likely owing
33 to two major factors. First, treatment-related toxicity increases
34 with age, which prevents the use of intensive chemotherapy
35 (1, 5). Second, adult B-ALL have decreased sensitivity to treat-
36 ments when compared with children due to different leuke-
37 mia genomic backgrounds. Hence, large genomic studies have
38 highlighted the age-related prevalence of distinct genetic aber-
39 rations, with a drop in low-risk abnormalities (i.e., high hyper-
40 diploidy and *ETV6::RUNX1*) beyond the age of 10, together with
41 the progressive increase in high-risk subtypes, i.e., *BCR::ABL1*,
42 *BCR::ABL1*-like, *KMT2A*-rearranged and low hypodiploidy (6-9).
43 Therefore, a better understanding of the pathogenesis of high-
44 risk adult B-ALL is needed to improve clinical management.

45 B-ALL with low hypodiploidy (LH-ALL) is a distinct
46 entity primarily defined by karyotype harboring 32 to 39

47 chromosomes with a nonrandom pattern of chromosome
48 losses (10). Afterward, this entity was renamed “low hypo-
49 diploidy/near triploidy” to include cases with duplicated
50 low-hypodiploid genome sharing the same poor prognosis
51 (11). Within childhood B-ALL, LH-ALL represents a very
52 small subset associated with a dismal outcome despite being
53 treated with the most intensive procedures (12). A previous
54 study in pediatric ALL showed that most LH-ALL harbored
55 *TP53* mutations, with half of them being of germline origin,
56 connecting LH-ALL to the spectrum of the Li-Fraumeni
57 cancer-predisposing syndrome (13). In adults, LH-ALL is also
58 associated with poor outcomes (8) and frequent *TP53* muta-
59 tions (14-16), but few data addressed the somatic origin of
60 *TP53* mutations.

61 Clonal hematopoiesis is a condition characterized by the
62 clonal expansion of hematopoietic stem/progenitor cells
63 (HSPC) carrying somatic mutations at detectable levels.
64 Sequencing of large cohorts of healthy subjects has shown
65 that the prevalence of clonal hematopoiesis increased con-
66 tinuously with age, defining age-related clonal hematopoiesis
67 (ARCH; refs. 17-19). Importantly, *TP53* is one of the most

68 frequent genes involved in ARCH. In addition, *TP53*-mutant
69 clonal hematopoiesis is associated with an increased risk of
70 developing myeloid malignancies, including secondary and
71 treatment-related myeloid neoplasms (20–22).

72 Here, we identified and characterized a large cohort of
73 adults with LH-ALL. Then, considering the dramatically
74 increased proportion of LH-ALL with age, we sought to investi-
75 gate the possible role of *TP53*-mutant clonal hematopoiesis
76 in the pathogenesis of adult LH-ALL. Using paired diagnosis/
77 remission samples and a single-cell multiomics platform, we
78 demonstrate that LH-ALL can arise from a preleukemic *TP53*-
79 mutant HSPC clone.

80 RESULTS

81 DNA Sequencing–Based Assessment of Copy- 82 Number Aberrations and Loss-of-Heterozygosity 83 Is Critical for Identifying LH-ALL

84 We studied a prospective cohort of adults with newly diag-
85 nosed Philadelphia (Ph)-negative B-ALL with available diag-
86 nostic sample ($n = 591$; Fig. 1A). We used targeted-capture
87 sequencing to carry out copy-number aberrations (CNA)
88 analysis and classified cases by a modal chromosomal num-
89 ber based on both karyotype and CNA data (Fig. 1B; Supple-
90 mentary Fig. S1A and Supplementary Table S1). Noticeably,
91 hypodiploid leukemic cells can sometimes undergo endorep-
92 lication, leading to a high number of chromosomes. There-
93 fore, we examined all the cases presenting with either ≤ 40
94 ($n = 41$) or ≥ 50 chromosomes ($n = 87$). All cases with ≤ 40 chro-
95 somes corresponded to LH-ALL, except one having near
96 haploidy, confirming that the latter corresponds to a subtype
97 virtually not found in adult ALL. Within cases with ≥ 50 chro-
98 somes, loss-of-heterozygosity (LOH) analysis enabled to
99 identify cases with a duplicated low-hypodiploid genome, as
100 harboring multiple uniparental disomies corresponding to
101 the same pattern as that of chromosome losses in classic low
102 hypodiploidy (Supplementary Fig. S1B). Importantly, LOH
103 analysis unequivocally distinguished duplicated low hypo-
104 diploidy from high hyperdiploidy, the latter corresponding
105 to a distinct good-risk B-ALL subtype.

106 Nearly half (40/87, 46%) of all cases with ≥ 50 chromosomes
107 turned out to have a duplicated low-hypodiploid genome
108 (Fig. 1C). The ancestral low-hypodiploid clone was detectable by
109 karyotype in only a few patients (5/40, 13%; Fig. 1D), suggesting
110 that they could have been misclassified as high hyperdiploidy
111 based on cytogenetics only. Moreover, in 26 of 80 cases (33%)
112 eventually classified as LH-ALL, conventional cytogenetics con-
113 cluded to culture failure or normal karyotype, suggesting that
114 leukemic cells failed to grow *in vitro*. We also identified two
115 LH-ALL cases as having the canonical pattern of chromosome
116 losses, albeit with a modal chromosome number >39 due to
117 trisomy 21. Therefore, our data illustrate that CNA and LOH
118 analyses are critical to allocate correctly B-ALL to distinct ane-
119 ploidies representing clinically relevant B-ALL subtypes.

LH-ALL Represents a Major B-ALL Subtype in Older Adults

120 Overall, combined cytogenetic and molecular analyses of
121 591 Ph-negative B-ALL adult patients identified 80 patients
122 with LH-ALL (13.5%), either harboring classic low hypodiploidy
123 ($n = 40$) or duplicated low hypodiploidy ($n = 40$). We analyzed
124 the baseline characteristics of LH-ALL patients with regard to all
125 the other Ph-negative B-ALL from adult patients (Table 1). LH-
126 ALL patients were significantly older than other B-ALL patients
127 (median 59 vs. 39 years, $P < 0.0001$) and there was a dramatic
128 increase in LH-ALL prevalence with age, ranging from 3% (8/267)
129 in patients below the age of 40 to 32% (55/171) in patients over
130 55 years. Other distinct features of LH-ALL included a lower
131 white blood cell count (3.2 vs. 7.5 G/L, $P < 0.001$) and a lower
132 marrow blast infiltration (79 vs. 92%, $P < 0.001$). Overall, LH-
133 ALL represents a large fraction of adult Ph-negative B-ALL and
134 has an age-related distribution, from being rare in young adults
135 to become very common in older patients.

Adult LH-ALL Exhibits *TP53* Biallelic Alteration and a Distinct Pattern of Chromosomal and Gene Abnormalities

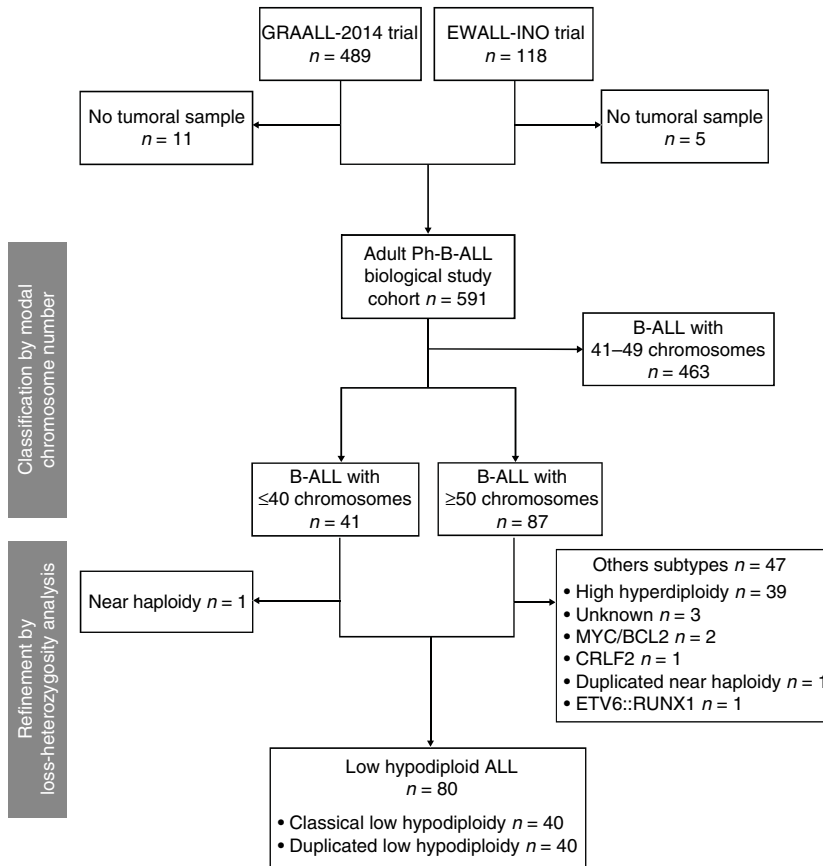
138 We performed targeted DNA sequencing (DNA-seq) of a
139 panel of genes recurrently altered in B-ALL and integrated
140 karyotype, CNA, LOH, and mutation data to characterize the
141 full spectrum of genomic alterations in adult LH-ALL. The
142 pattern of chromosome losses was highly recurrent, includ-
143 ing chromosomes 3, 7, 16, and 17 in virtually all cases and
144 chromosomes 13 and 15 in over 80% of cases, whereas chro-
145 somes 2, 4, 9, 12, and 20 were more variably lost, in half of
146 cases each (Fig. 1D; Supplementary Fig. S1C). Of note, chro-
147 some 21 was retained in all cases. In addition, structural
148 abnormalities were present in 31 of 80 (39%) cases.

149 We found *TP53* mutations in 78 of 80 (98%) cases (Fig. 2A;
150 Supplementary Table S2). They included missense, nonsense,
151 splice-site mutations, and short insertions/deletions, all pre-
152 dicted to be pathogenic (Fig. 2B). Monosomy 17 or uni-
153 parental disomy led to the loss of the second *TP53* allele
154 in all cases but one having biallelic *TP53* mutations. *TP53*
155 mutations were present at variant allele frequencies (VAF)
156 correlated with leukemic cell infiltration (Fig. 2C), suggest-
157 ing that alterations of both alleles were present in the major
158 clone. Noticeably, considering the whole cohort of adult Ph-
159 negative B-ALL, 76% (78/102) of patients with *TP53* mutation
160 had LH-ALL, whereas *TP53* mutations were rarely detected
161 in other B-ALL (5% vs. 98%, $P < 0.001$, two-tailed Fisher test;
162 Fig. 2D). Therefore, biallelic alteration of *TP53* is a hallmark
163 of LH-ALL within adult B-ALL.

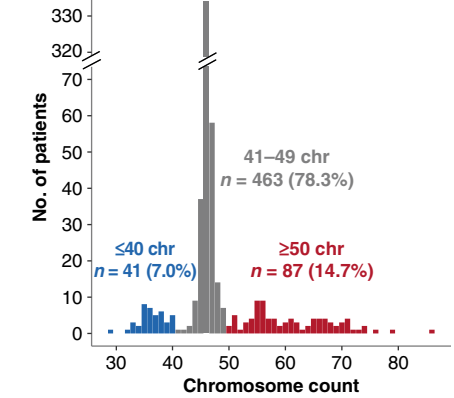
164 Alterations of genes involved in cell-cycle regulation defined
165 the second most frequently altered pathway. Specifically, focal
166 deletions and loss-of-function mutations in the *CDKN2A* and
167 *RB1* genes (Fig. 2A; Supplementary Fig. S2A), associated
168 with monosomies 9 and 13, led to biallelic inactivation in 21
169 (26%) and 18 (23%) cases, respectively, in a mutually exclusive
170

Figure 1. Identification of a cohort of 80 LH-ALL cases by karyotyping and sequencing-based assessment of CNA and LOH. **A**, Flow diagram describing the study cohort of Ph-negative B-ALL adult patients. **B**, Distribution of B-ALL cases according to their modal chromosome number assessed by karyotyping and/or sequencing-based CNA analysis. **C**, Proportion of LH-ALL within cases with ≤ 40 chromosomes and cases with ≥ 50 chromosomes after integration of sequencing-based LOH analysis. **D**, Heat map of chromosome anomalies as determined by karyotyping or CNA/LOH analysis in the 80 LH-ALL cases.

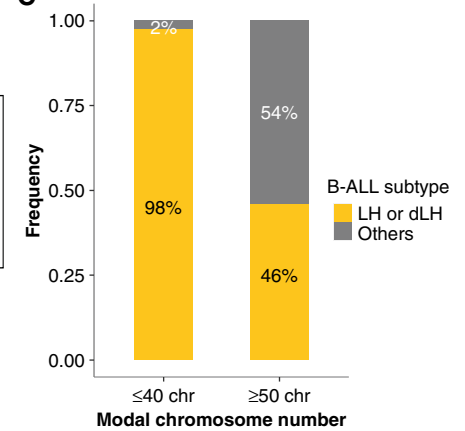
A



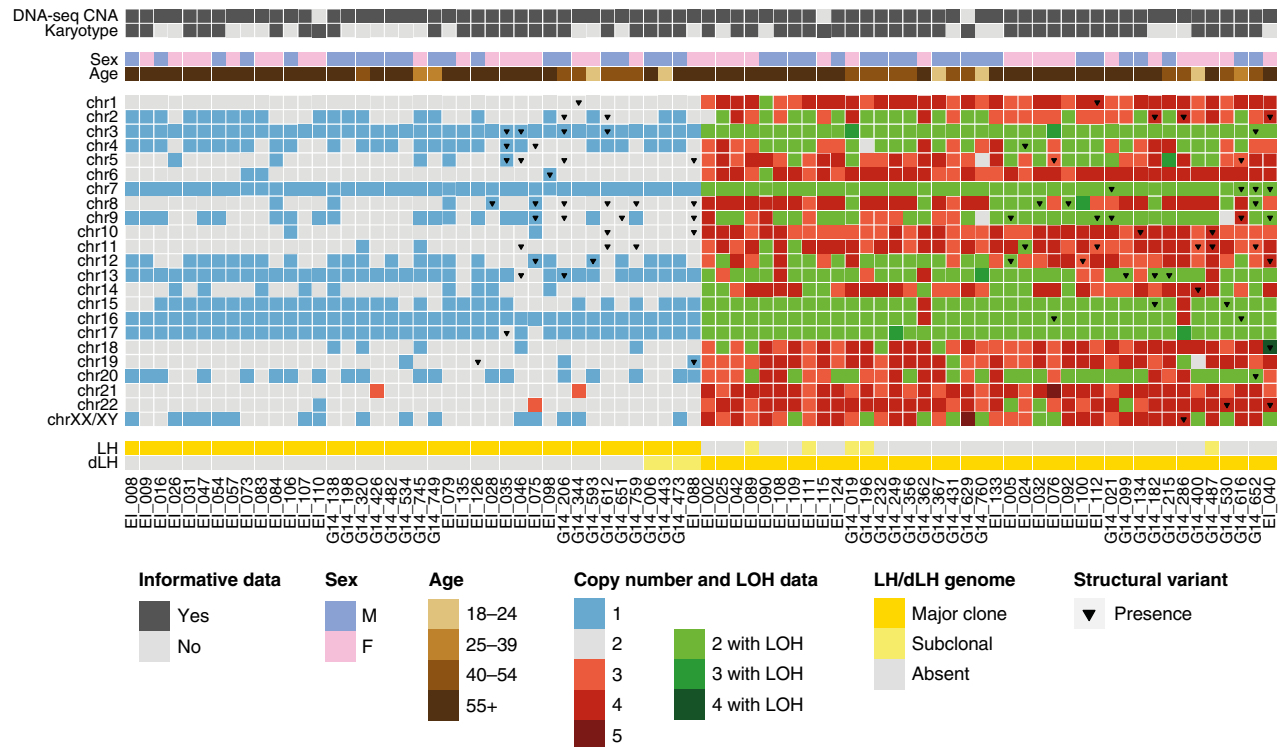
B



C



D



Downloaded from <http://aacrjournals.org/bloodcancerdiscovery/article-pdf/doi/10.1158/2643-3230.BCD-22-0154/3269427/bcd-22-0154.pdf> by guest on 26 September 2023

Table 1. Demographic and clinical characteristics of patients at baseline.

	LH-ALL	Non LH-ALL	P
Patients, n	80	511	
Sex, n (%)			
Male	42 (53)	269 (53)	1
Female	38 (47)	242 (47)	
Age, year			
Median	59	39	<0.0001
Range	18–84	18–84	
Age group, n (%)			
18–24 y	5 (6)	123 (24)	<0.0001
25–39 y	3 (4)	136 (27)	
40–54 y	17 (21)	136 (27)	
≥ 55 y	55 (69)	116 (23)	
White blood cell count ^a , Giga per liter			
Median	3.2	7.5	<0.0001
Range	0.4–87.1	0.4–712.0	
Marrow blast infiltration ^b , %			
Median	79	92	<0.0001
Range	21–99	12–100	
CD10 expression ^c , n (%)			
Positive	62 (79)	382 (76)	0.67
Negative	16 (21)	118 (24)	

^aWhite blood cell counts were available for 582 patients.

^bMarrow blast cell counts were assessed for 569 patients.

^cCD10 expression was assessed by flow cytometry for 578 patients.

Two-tailed independent t tests and two-tailed Fisher tests were used for continuous and categorical variables, respectively, and statistical significance was defined as a $P < 0.05$.

173 pattern. The lymphoid transcription factor gene *IKZF2* was
174 recurrently affected by focal deletions, observed in 15 cases
175 (19%). By contrast, no intragenic deletion or mutation of
176 *IKZF1*, one of the most frequently altered genes in adult
177 B-ALL, was found, although hemizygoty was observed in all
178 cases as a result of monosomy 7. Similarly, *PAX5* was rarely
179 targeted by focal deletions or mutations (8%).

180 Aberrations involving cell signaling genes were present in
181 25 (31%) LH-ALL cases, including loss-of-function mutations
182 and focal deletions of *NF1* in 18 (23%) cases (Supplementary
183 Fig. S2B). We also identified *FLT3* mutations in 6 cases
184 (8%; Supplementary Fig. S2C), *NRAS* mutations in 3 cases
185 (4%), and remarkably, *JAK2* p.V617F mutation in one case
186 (EI_046). Finally, we detected *TET2* and *DNMT3A* mutations
187 corresponding to classic mutations reported in ARCH and
188 myeloid malignancies in 11% and 10% of cases, respectively
189 (Supplementary Fig. S2D–S2E).

190 Altogether, adult LH-ALL is characterized by a distinct
191 pattern of aneuploidy, consistent biallelic alteration of *TP53*,
192 and a constellation of additional gene alterations, the most
193 frequent involving *CDKN2A*, *RB1*, *NF1*, and *IKZF2*.

TP53 Mutations Are Detected at Remission in a Substantial Proportion of Adults with LH-ALL

194
195
196 Given the age-related distribution of LH-ALL and the role
197 of *TP53* mutations in ARCH, we hypothesized that LH-ALL
198 may be secondary to *TP53*-mutant ARCH. To test this hypoth-
199 esis, we looked for *TP53* mutations in posttreatment remis-
200 sion bone marrow samples assessed for minimal residual
201 disease (MRD). Among the 73 patients with available samples,
202 we observed persistence of the *TP53* mutation identified at
203 diagnosis in 25 patients (34%), at VAF ranging from 2.6% to
204 51.2% (cutoff value for positivity set at 2%; Fig. 3A and B; Sup-
205 plementary Table S3). *DNMT3A* and *TET2* mutations were
206 also detected in remission samples from 9 and 6 patients,
207 respectively. MRD levels based on the quantification of clonal
208 rearrangements of immunoglobulin or T-cell receptor genes
209 (*IG/TR*) were either undetectable or measured at much lower
210 levels (Supplementary Table S4), indicating that those muta-
211 tions were not related to residual B-ALL leukemic cells.

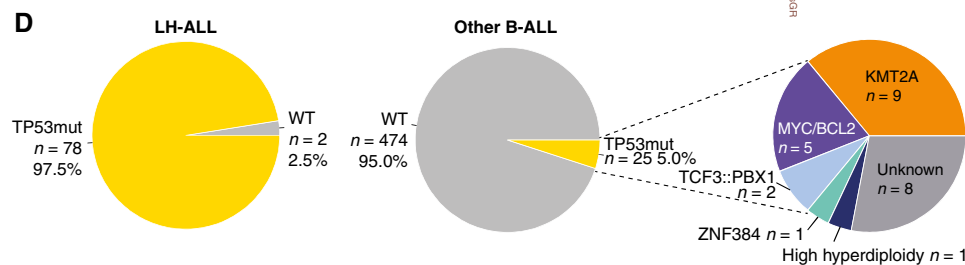
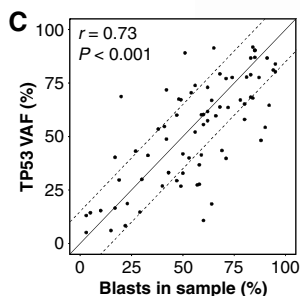
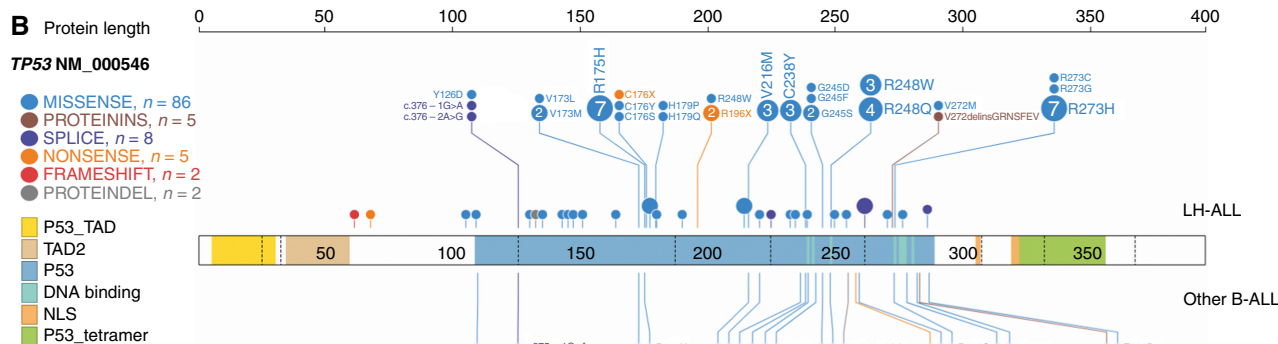
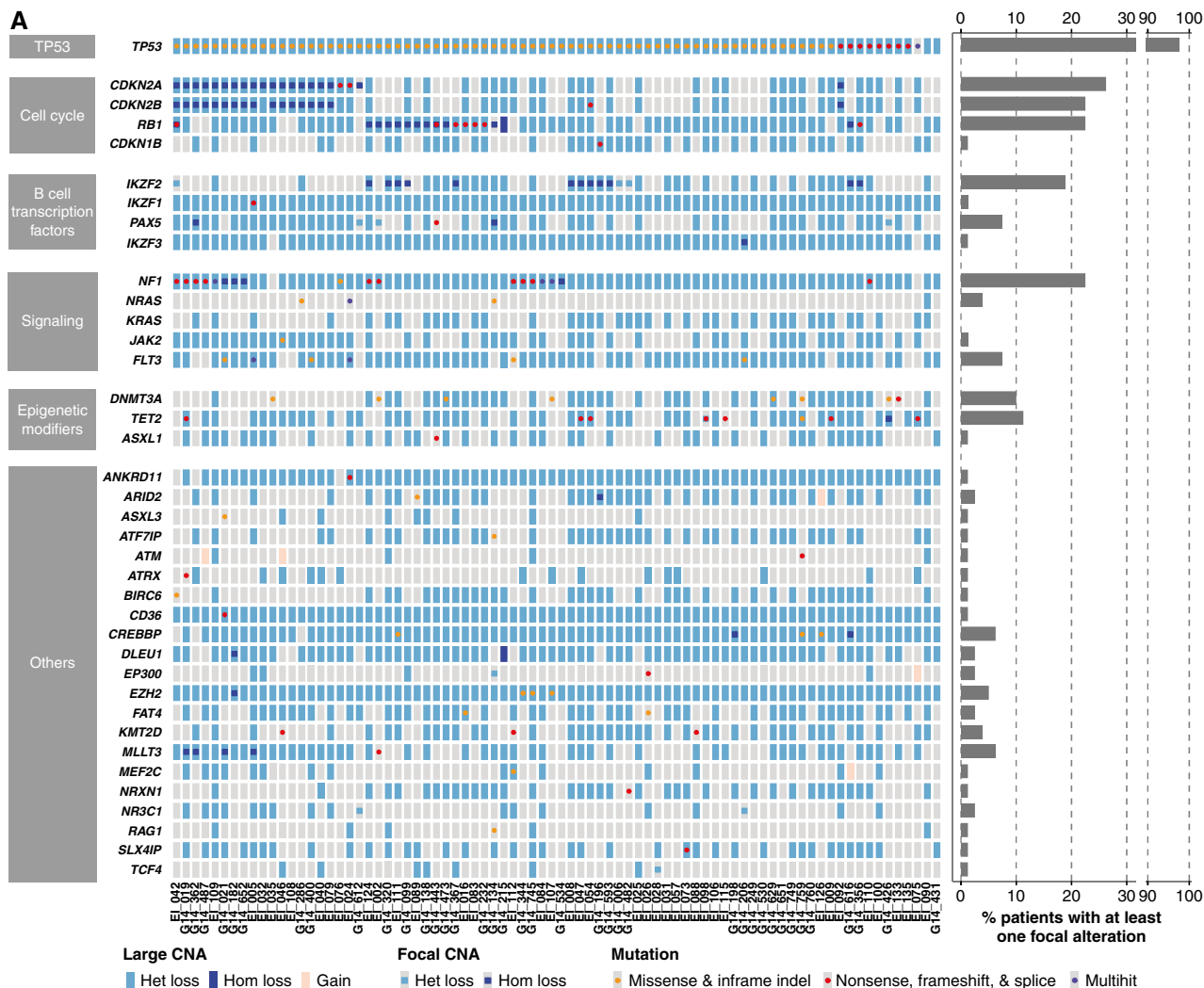
212 It should be noticed that 5 patients had a *TP53* mutation
213 with a VAF >40%, raising the possibility of a germline origin, as
214 previously observed in pediatric LH-ALL. This could be ruled
215 out in two patients for whom *TP53* mutation was not detected
216 in nonleukemic cells (Supplementary Table S3). In the three
217 remaining patients, including one with detectable *TP53* muta-
218 tion in sorted T cells and two without available nonleukemic
219 material, a germline origin could not be ruled out.

220 Next, to evaluate the dynamics of the *TP53*-mutant cell
221 fraction, we used digital droplet PCR (ddPCR) to quantify
222 *TP53* mutations in 9 patients with available longitudinal
223 postremission bone marrow samples (Fig. 3C; Supplementary
224 Fig. S3). In two patients with confirmed somatic *TP53* muta-
225 tion, the *TP53*-mutant clone remained in a steady state at
226 high rates at all time points. Four patients displayed a reduc-
227 tion of the *TP53*-mutant fraction over time, yet uncoupled
228 from lower or undetectable *IG/TR* MRD levels. Noticeably, in
229 two of these patients, the higher sensitivity of ddPCR allowed
230 to detect a low fraction of persistent *TP53*-mutant cells not
231 detected by sequencing. In three other patients, no *TP53*-
232 mutant cells were detected. Overall, these results reveal that a
233 substantial proportion of adults with LH-ALL carry somatic
234 *TP53* mutations in nonleukemic cells repopulating bone mar-
235 row after treatment.

Integrated Single-Cell Genotyping and Immunophenotyping Reveals Multilineage TP53-Mutant Clonal Population at Remission Stage

236
237
238 We sought to investigate the contribution of the *TP53*-
239 mutant clone to the different hematopoietic lineages and
240 infer the oncogenic route toward LH-ALL. Using antibody-
241 derived tag (ADT) sequencing and a custom single-cell DNA-
242 seq (scDNA-seq) panel (23–25), we performed simultaneous
243 single-cell immunophenotyping and genotyping on three
244 bone marrow specimens obtained after induction. The three
245

Figure 2. Landscape of recurrent genomic alterations in adult LH-ALL. **A**, Heat map of recurrent CNA and mutations in the 80 LH-ALL cases. Focal alterations refer to CNA not involving whole chromosome arms and mutations. Cases with several mutations are referred to as multihit. **B**, Lollipop plot depicting *TP53* mutations detected in both LH-ALL and other Ph-negative B-ALL. **C**, Correlation between *TP53* mutation VAF and blast percentage, as assessed by flow cytometry after ficoll or morphology on marrow smear, using Pearson correlation coefficient. **D**, Proportion of *TP53* mutations in LH-ALL and other Ph-negative B-ALL with available data from the study cohort ($n = 499$). Het, heterozygous; Hom: homozygous; indel: insertion/deletion.



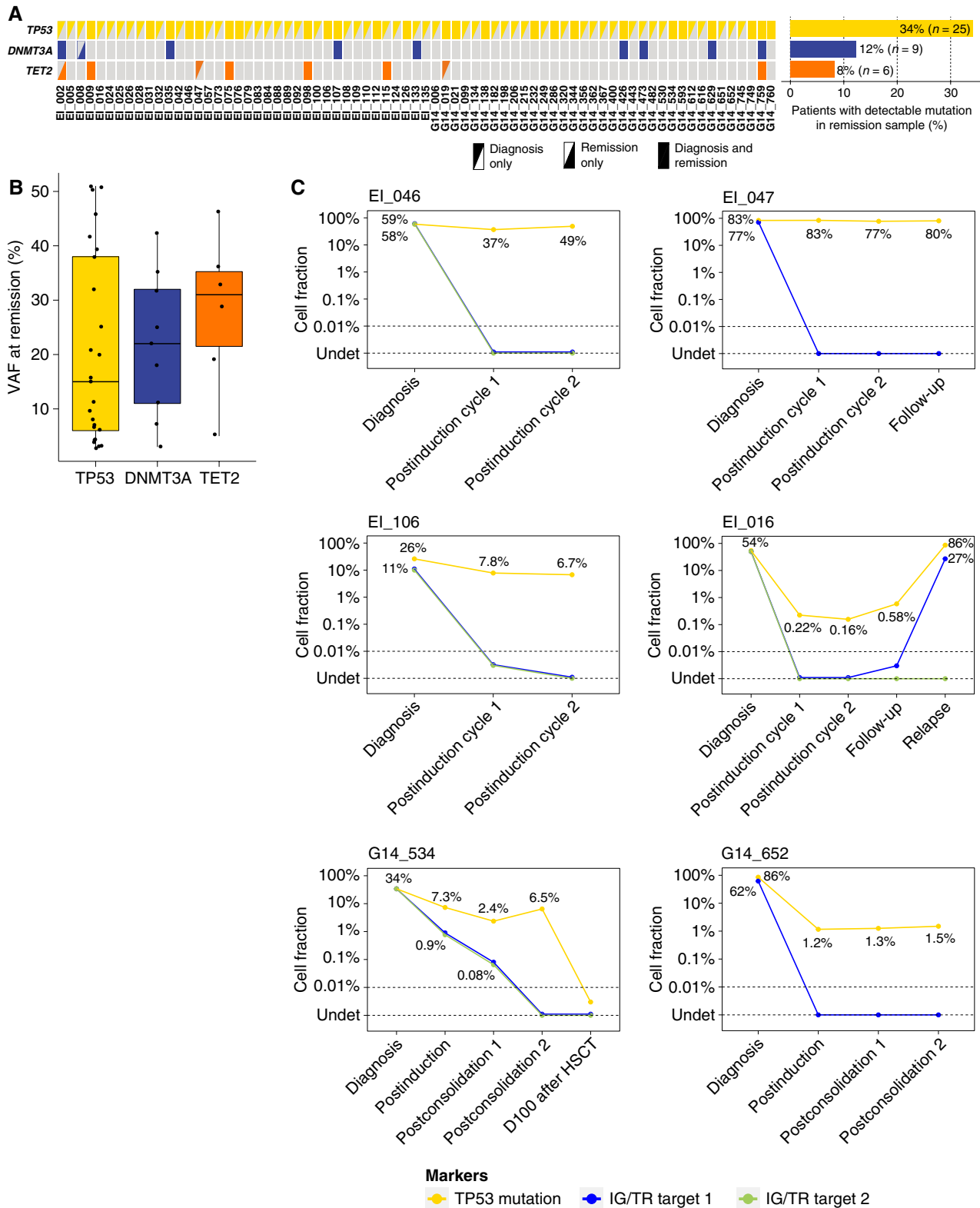


Figure 3. Tracking of ARCH-related mutations in remission samples of LH-ALL patients. **A**, Heat map of mutations in paired diagnosis and remission samples for 71 patients. Data are based on sequencing data with a threshold for positivity at 2% VAF. **B**, Box plot for VAF of mutations detected by sequencing at remission. **C**, Longitudinal assessment of *TP53*-mutant cell fraction as determined by ddPCR (0.05–0.1% sensitivity), along with clonal *IG/TR*-based MRD quantification (0.01%–0.001% sensitivity), for six patients with *TP53* mutation detected in remission samples, including two below the sequencing detection threshold.

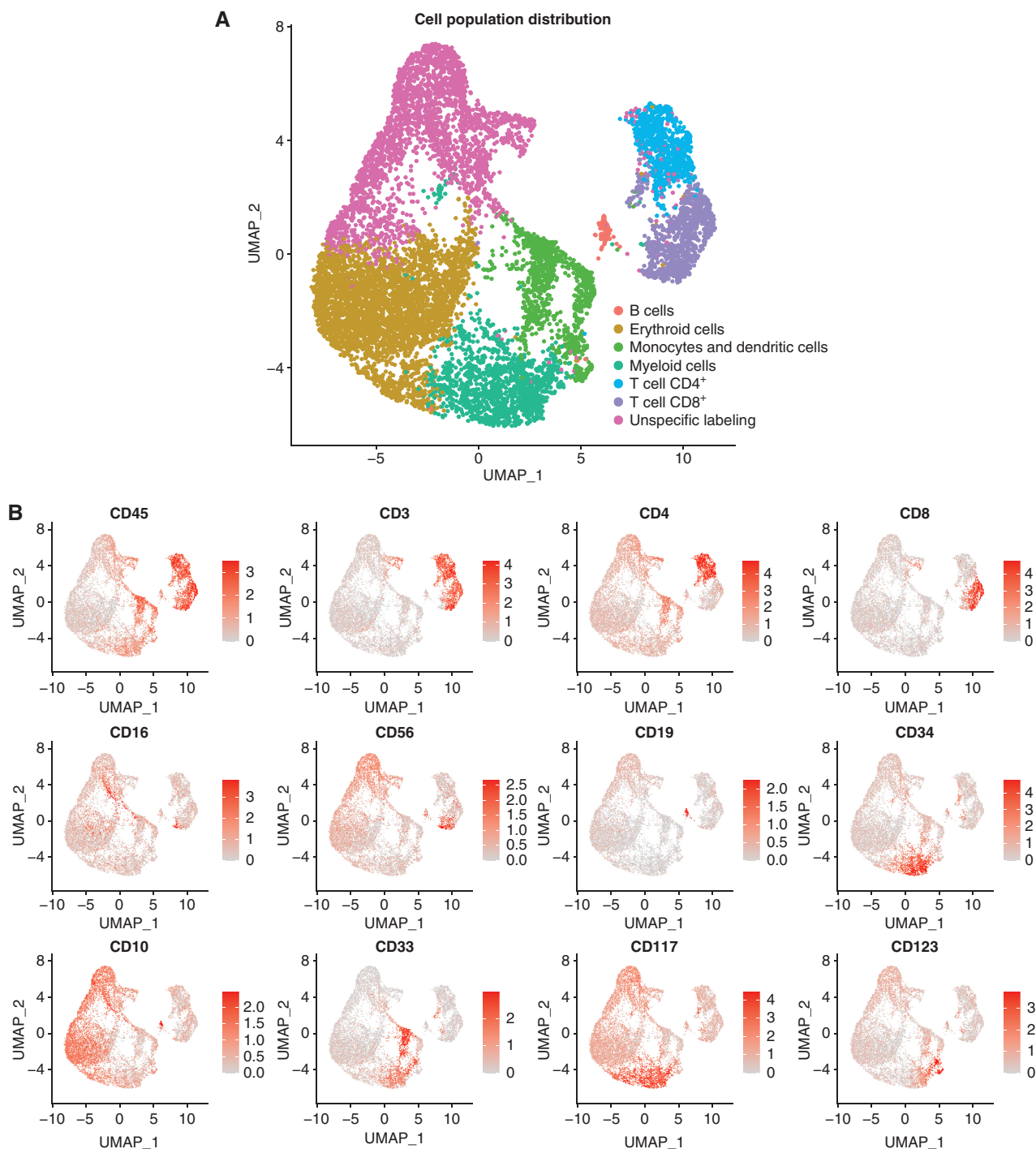


Figure 4. Integrated single-cell genotyping and immunophenotyping reveal a multilineage *TP53*-mutant clonal population at the remission stage in LH-ALL patients. **A**, Uniform Manifold Approximation and Projection (UMAP) plot of 10,598 cells from remission samples of three patients (E1_047, E1_031, and E1_035 having 1,017, 5,450, and 4,131 cells available for analysis, respectively). Cells are clustered by expression of cell-surface markers and colored according to assigned clusters. **B**, Same UMAP plots with cells colored by expression of specific cell-surface markers used to assign cell clusters. (continued on next page)

246 patients were treated in the EWALL-INO trial and had a *TP53*
 247 mutation detected at postinduction remission, whereas MRD
 248 measured on the same sample was either low or undetectable.
 249 Protein expression data allowed discrimination of 7 distinct
 250 clusters (Fig. 4A). Based on lineage-specific markers, we

were able to identify confidently T cells, B cells, monocytes,
 dendritic cells (DC), and myeloid and erythroid cell clusters
 (Fig. 4B; Supplementary Fig. S4A and S4B). Cell identity
 could not be assigned to the remaining cluster owing to
 unspecific and weak labeling of frail cells (thereafter named

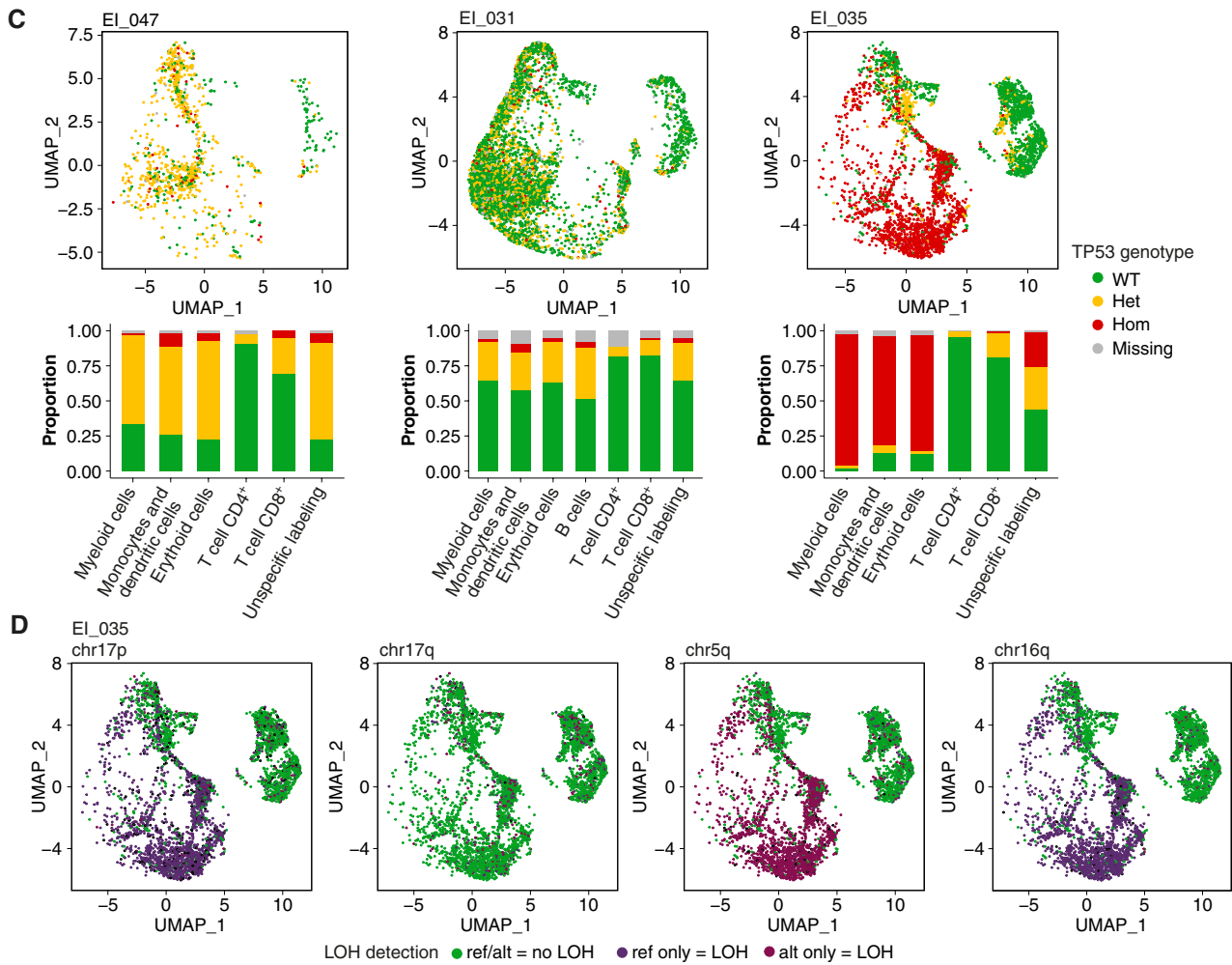


Figure 4. (Continued) C, Same UMAP plots (top) for individual patient's remission samples, with cells colored according to *TP53* genotype. Histograms (bottom) show the proportion of each *TP53* genotype within each cell cluster. **D,** UMAP plots for the EI_035 remission sample, with cells colored according to genotype for several heterozygous SNPs allowing LOH assessment. ref, reference allele; alt, alternative allele.

256 “unspecific labeling”). Of note, few B cells were detected, 257 which may be related to therapy including B cell-directed 258 antibodies. Cell type composition was comparable across 259 patients, but analyses on each sample individually allowed 260 better identification of discrete cell populations not detected 261 in all patients, such as natural killer (NK) cells and plasmacy- 262 toid dendritic cells (pDC; Supplementary Fig. S5).

263 Projection of the *TP53* genotype on the protein uniform 264 manifold approximation and projection (UMAP) repre- 265 sentation allowed us to describe the cell architecture of 266 the *TP53*-mutant clone (Fig. 4C; Supplementary Fig. S6). 267 Patients EI_031 and EI_047 had similar patterns with *TP53*- 268 heterozygous mutant cells detected in substantial fractions of 269 myeloid, erythroid, and monocyte/DC clusters (hereafter col- 270 lectively named myeloid clusters). The “unspecific labeling” 271 cluster was likely related to myeloid populations according 272 to the similar proportion of mutant cells. T-cell populations 273 also contained mutant cells, yet at lower rates. For patient 274 EI_031, NK cells, pDC, and B-cell clusters could be identi- 275 fied and also harbored mutant cells. Of note, the observation 276 of rare cells with a homozygous genotype was likely related

277 to allelic dropout and biologically not relevant, in agree- 278 ment with similar proportions observed for constitutional 279 heterozygous single-nucleotide polymorphisms (SNP; Sup- 280 plementary Fig. S7).

281 Patient EI_035 harbored a large fraction of cells in 282 myeloid clusters carrying *TP53*-homozygous mutation, 283 pinpointing a concomitant CNA or copy-neutral LOH in 284 those cells. By contrast, T cells were mainly wild-type, with 285 a minority being heterozygous. Including amplicons cover- 286 ing common SNPs in the scDNA-seq panel allowed us to 287 investigate allelic imbalance throughout the genome at the 288 single-cell level. Thus, we evidenced LOH at 17p (but not 289 at 17q) in myeloid clusters, suggesting a cytogenetic aber- 290 ration at 17p resulting in the loss of the wild-type allele 291 (Fig. 4D; Supplementary Fig. S8). Those cells also had 292 LOH at 5q and 16q, whereas no other LOH possibly related 293 to the LH-ALL clone was observed. Thus, the presence of 294 those aberrations restricted to the myeloid compartments 295 may be related to a distinct, myelodysplastic clone, only 296 sharing the *TP53* alteration with the LH-ALL clone. Alto- 297 together, these results show that patients with LH-ALL carry

298 *TP53*-mutant HSPCs able to repopulate bone marrow after
299 intensive treatment.

300 **LH-ALL Arises from Preexisting *TP53*-Mutant** 301 **Clonal Hematopoiesis**

302 We next aimed to address whether the *TP53*-mutant multi-
303 lineage cell population arose from clonal selection under the
304 stress of cytotoxic therapy for B-ALL or preexisted at diagnosis.
305 We profiled 14,518 cells from three diagnostic samples,
306 including two paired with remission samples already presented
307 (EI_047 and EI_035). ADT-sequencing and *IG/TR* clono-specific
308 sequences enabled to recognize B-ALL leukemic cells and
309 to identify minor nonleukemic cell populations (Fig. 5A and
310 B; Supplementary Fig. S9). In B-ALL cells from the 3 patients,
311 *TP53* and SNP single-cell genotyping showed homozygous
312 (hemizygous) *TP53* mutation and LOH at multiple loci
313 (Fig. 5C; Supplementary Fig. S10), in agreement with bulk
314 data (Fig. 1D; Supplementary Table S2). In EI_046 and EI_047,
315 substantial fractions of *TP53*-heterozygous mutant cells were
316 observed within myeloid and NK cell populations, as observed
317 in the paired-remission sample of EI_047. Similarly, in EI_035,
318 the myeloid population was predominantly *TP53*-homozygous
319 mutant. By contrast, the small subset of *TP53*-heterozygous
320 mutant T cells was likely related to the cell doublet artifact,
321 in agreement with a similar rate of detection of clonal *IG/TR*
322 rearrangements (Supplementary Table S5). Consistent results
323 were obtained through analyses of the fluorescence-activated
324 cell sorting (FACS) of cell fractions (Supplementary Table S6).

325 Overall, these results confirm that the *TP53*-mutant mye-
326 loid population preexisted at B-ALL diagnosis and indicate
327 that *TP53*-mutant ARCH likely preceded the onset of B-ALL.

328 **Other ARCH-Related Genes Can Be Involved in the** 329 **Pathogenesis of LH-ALL**

330 Because other ARCH-related mutations were identified in
331 bulk diagnostic samples from several patients with LH-ALL,
332 we aimed to investigate their relation with *TP53*-mutant
333 clonal hematopoiesis and LH-ALL and decipher the sequence
334 of mutation acquisition.

335 EI_047 had a *TET2* mutation detected in bulk sequencing at
336 diagnosis at 48% VAF. Unexpectedly, single-cell analysis of the
337 diagnosis sample revealed that this mutation was restricted
338 to B-ALL cells and was not carried by myeloid cells (Fig. 6A).
339 Accordingly, it was not detected in the bulk remission sample.

340 EI_046 harbored a *JAK2* V617F detected at 7% VAF in the
341 bulk diagnosis sample. Single-cell analysis revealed that it was
342 restricted to myeloid and erythroid cells, in a homozygous
343 state, reminiscent of myeloproliferative neoplasms (MPN).
344 Moreover, the *TP53* and *JAK2* mutations appeared to be in
345 independent clones, as no cell carried both mutations (Sup-
346 plementary Fig. S11). Therefore, single-cell analysis uniquely
347 evidenced a *JAK2*-mutant ARCH or MPN-like clone, concomi-
348 tant but clonally unrelated to B-ALL.

349 EI_035 had a *DNMT3A* mutation at diagnosis (VAF 45%),
350 still detected at remission (VAF 42%). Single-cell analysis
351 of the diagnosis sample showed that almost all B-ALL and
352 nonleukemic cells carried heterozygous *DNMT3A* mutation.
353 The presence of *TP53*-wild-type *DNMT3A*-mutant cells in the
354 remission sample (Supplementary Fig. S11) indicated that
355 *DNMT3A* mutation occurred earlier than *TP53* mutation. In

addition, and as observed at remission, myeloid cells had LOH 356
at 5q, 16q, and 17p, suggesting a premalignant, concurrent 357
clone at B-ALL diagnosis (Fig. 6B). All B-ALL cells had LOH at 358
these loci and at additional loci in relation with low hypodip- 359
loidy. However, the discordant homozygous genotype at 16q 360
between B-ALL and myeloid cells indicated a branched rather 361
than linear relation between the myeloid and B-ALL clones. 362

Overall, these data allow to reconstruct the sequence of 363
mutation acquisition (Fig. 6C) and show that adult LH-ALL 364
can develop on a background of clonal hematopoiesis resem- 365
bling myelodysplastic syndrome (MDS) or MPN. 366

367 **DISCUSSION**

368 Our study establishes a comprehensive genomic charac- 369
terization of the largest series of LH-ALL reported so far. 370
By combining sequencing-based CNA and LOH analyses to 371
cytogenetics data in a prospective cohort of 591 Ph-negative 372
adult ALL, we identified a high proportion of LH-ALL, reach- 373
ing 32% in the older range of patients. This increased preva- 374
lence in older adults is in agreement with, but higher than, 375
that observed in previous studies, including the recent UKALL 376
study of older adult ALL (9). Although the diagnostic pitfall 377
of duplicated hypodiploidy/near triploidy is recognized, our 378
data suggest that a number of LH-ALL cases are still being 379
missed or misclassified owing to misleading normal or hyper- 380
diploid karyotypes. Hence, CNA/LOH analyses in our study 381
allowed to rescue more than a quarter of LH-ALL cases with 382
normal/failed karyotype, whereas duplicated low hypodip- 383
loidy represented up to half of all LH-ALL. Of note, we also 384
showed that LH-ALL patients present with lower blast counts 385
in bone marrow and peripheral blood at diagnosis, which 386
may explain underrepresentation in retrospective molecular 387
studies relying on frozen samples. These findings warrant the 388
implementation of CNA/LOH analysis in diagnostic labora- 389
tory practices, because genetic classification is critical for risk- 390
adapted treatment stratification in most modern pediatric 391
and adult clinical trials. The improved genetic assignment will 392
also allow the refinement of future clinical correlation studies.

393 Our single-cell sequencing data on diagnostic and remission 394
samples indicate that *TP53* mutation is a preleukemic event 395
preceding aneuploidy with monosomy 17 leading to the loss of 396
the *TP53* wild-type allele. Although a dominant-negative effect 397
of *TP53* missense mutations has been proposed to mediate the 398
nonmutational inactivation of wild-type *TP53* (26), it is note- 399
worthy that genomic alteration of the second allele seems to be 400
mandatory in the pathogenesis of LH-ALL. The specific pattern 401
of chromosomal losses in adult LH-ALL, including the core 402
association of 3, 7, 16, and 17 monosomies, is consistent with 403
that observed in childhood LH-ALL and may inform about key 404
genes involved in LH-ALL oncogenesis. Loss of chromosome 7 405
results in haploinsufficiency for *IKZF1*, a critical gene for normal 406
B-cell differentiation, the recurrent loss of which in B-ALL drives 407
a pejorative impact (27). Chromosome 16 contains *CREBBP*, 408
which is also targeted by focal alterations in B-ALL, especially in 409
relapsed cases (28). Noteworthy, as the *CD19* gene is also located 410
on chromosome 16, LH-ALL having only one allele may be 411
prone to CD19 expression loss in the context of selective pres- 412
sure with CD19-directed therapeutic agents (29). Chromosome 413
3 contains several tumor suppressor genes previously shown

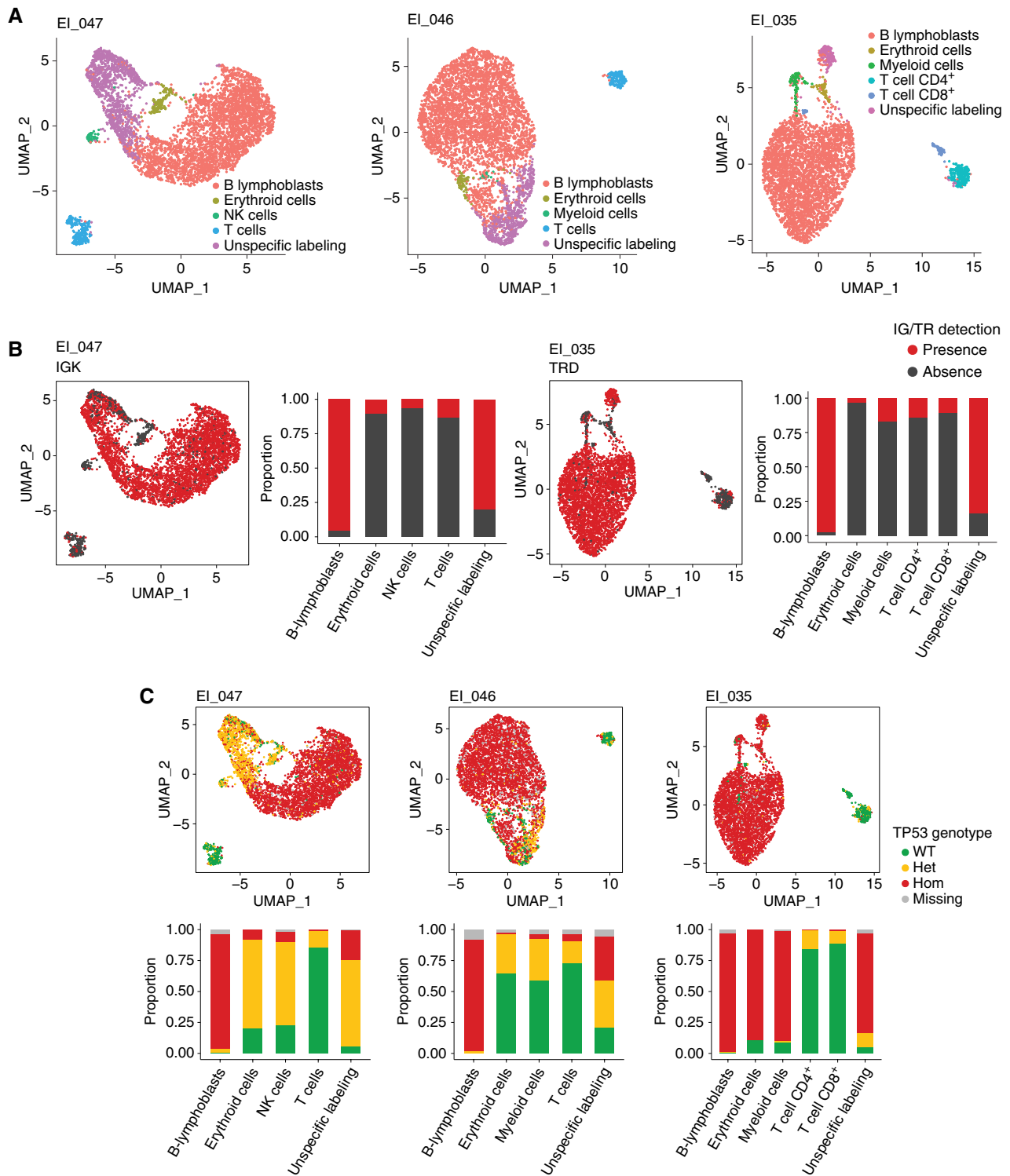


Figure 5. Single-cell analysis at LH-ALL diagnosis identifies a preexisting multilineage *TP53*-mutant clonal population. **A**, UMAP plots for individual diagnostic samples from three patients (EI_47, EI_46, and EI_035), having 5,228, 4,947, and 4,343 cells available for analysis, respectively. Cells are clustered by expression of cell-surface markers and colored according to assigned clusters. **B**, Same UMAP plots for patients EI_047 and EI_035, with cells colored according to the presence of specific clonal IG/TR sequences allowing to identify B-ALL cells. Histograms show the proportion of positive cells within each cell cluster. **C**, Same UMAP plots (top) with cells colored according to *TP53* genotype. Histograms (bottom) show the proportion of each *TP53* genotype within each cell cluster.

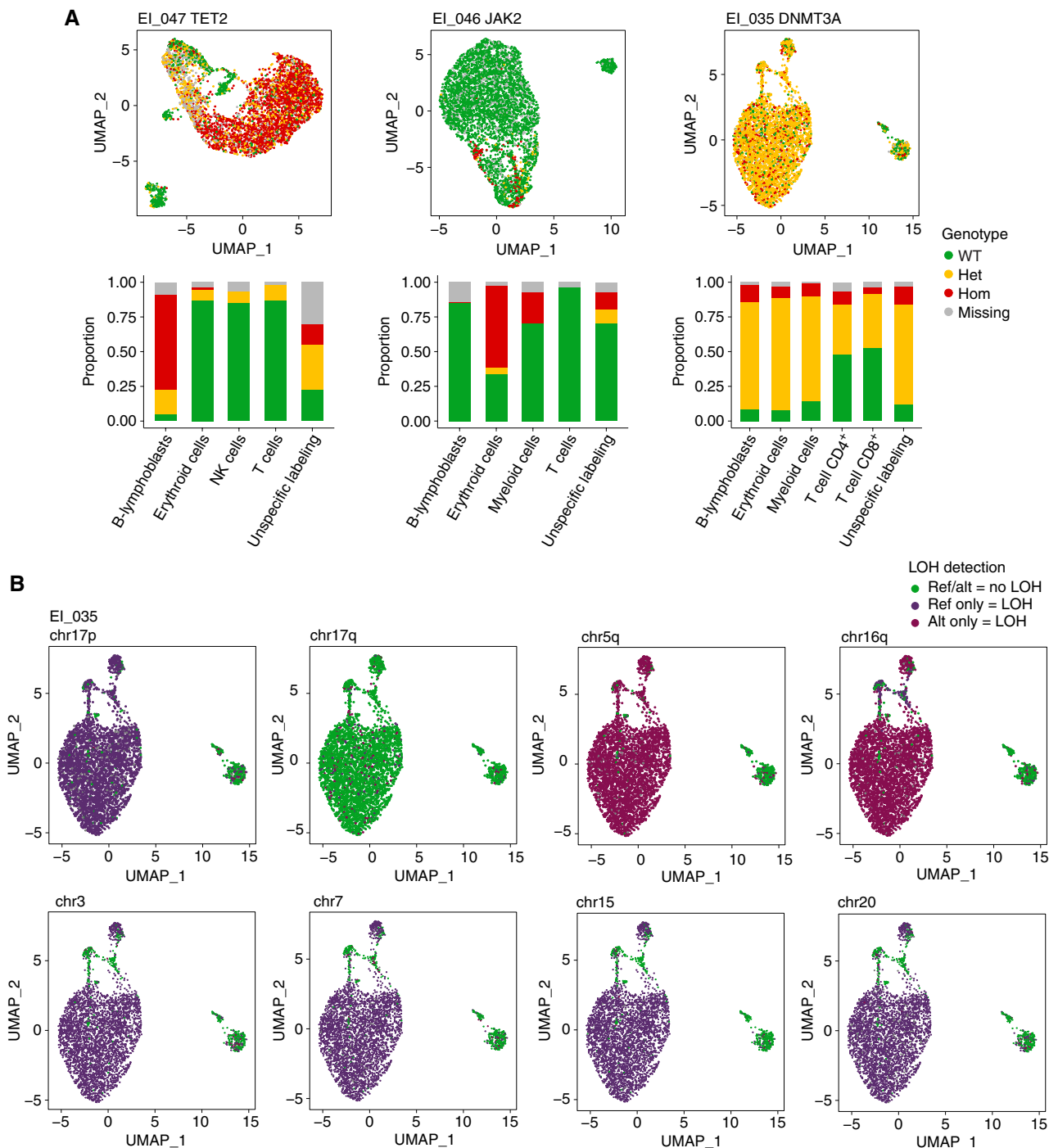


Figure 6. Integration of ARCH mutations into the clonal architecture of LH-ALL. **A**, UMAP plots for individual diagnostic samples from three patients with cells clustered by expression of cell-surface markers and colored according to genotypes of *TET2*, *JAK2*, and *DNMT3A* mutations in EI_047, EI_046, and EI_035, respectively. Histograms show the proportion of each genotype within each cell cluster. **B**, UMAP plots for the EI_035 diagnostic sample, with cells colored according to genotype for several heterozygous SNPs allowing LOH assessment. (continued on next page)

414 to be involved in B-ALL, i.e., *CD200/BTLA* locus and *SETD2*
 415 (27, 30, 31). Thus, by occurring at once, all these monosomies
 416 resulting in the loss of several key tumor suppressor genes may
 417 drive transformation and shape the tumor biology of LH-ALL.
 418 Additionally, this combinatorial pattern could also be the result

of the counter-selection of other aneuploidies possibly lethal to
 the target cell.

The genomic profiling of LH-ALL evidenced additional
 recurrent alterations in LH-ALL. Frequent and mutually
 exclusive alterations of the cell-cycle genes *CDKN2A* and *RB1*

419
 420
 421
 422
 423

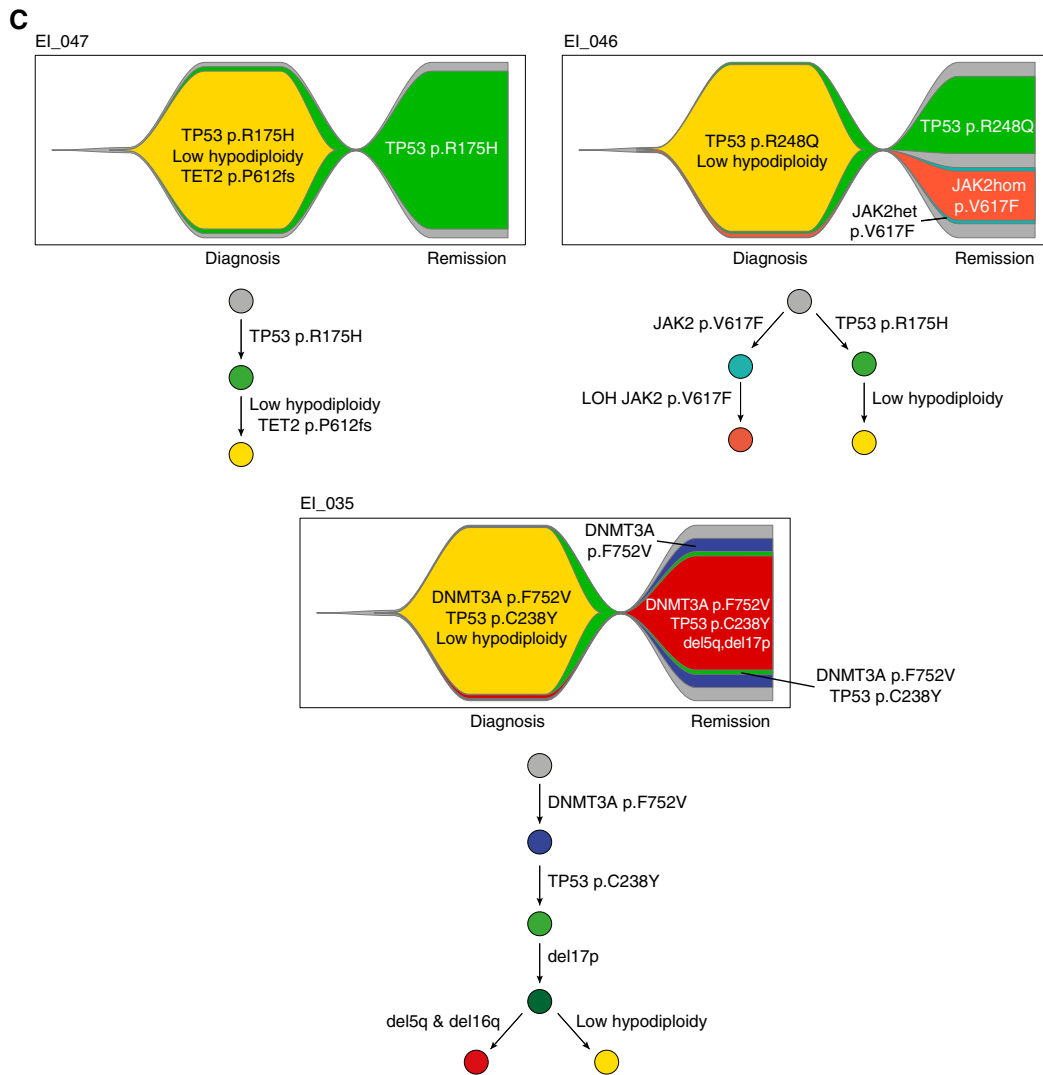


Figure 6. (Continued) C. Fish plots and phylogenetic trajectories depicting the clonal architecture and the sequential acquisition of genetic abnormalities.

424 suggest their functional redundancy and an oncogenic coop- 443
 425 eration with a *TP53*-deficient background. We identified *NF1* 444
 426 as a frequent target gene in adult LH-ALL, whereas it was not 445
 427 observed in their pediatric counterpart (13). 446

428 *DNMT3A* and *TET2* were among the top mutated genes, 447
 429 found in 10% of patients. As these genes are the most fre- 448
 430 quently mutated in ARCH (17), these mutations may simply 449
 431 reflect the older age of LH-ALL patients. Single-cell analy- 450
 432 s revealed different possible clonal involvement of those 451
 433 mutations not inferred by bulk sequencing. In one patient, 452
 434 *DNMT3A* mutation was the earliest somatic event, found in 453
 435 an ancestral multilineage hematopoietic clone, as previously 454
 436 shown in acute myeloid leukemia (AML; ref. 32). By contrast, 455
 437 in another patient, *TET2* mutation was found as a secondary 456
 438 genetic event restricted to leukemic cells, suggesting an unan- 457
 439 ticipated oncogenic role of *TET2* in B-ALL. In addition, in one 458
 440 patient with *JAK2* V617F mutation detected in bulk diagno- 459
 441 sis, the single-cell analysis demonstrated that it was clonally 460
 442 unrelated to *TP53*-mutant ALL cells, which is reminiscent 461

of post-MPN *TP53*-mutant AML lacking the MPN driver 443
 mutation (33). 444

445 The major finding of our study is that *TP53* mutations are not 446
 447 only frequently associated with LH-ALL, but they are indispen- 448
 449 sable genetic events preceding aneuploidy. Hence, we detected 449
 450 *TP53* mutations in virtually all LH-ALL cases and demonstrated 450
 451 that *TP53*-mutant heterozygous cells constituted a preleukemic 451
 452 compartment. This oncogenic route relying on initiating *TP53* 452
 453 mutation is thus distinct from that observed in other malignan- 453
 454 cies, including ALL (34), where *TP53* mutations often occur 454
 455 during tumor progression as a late event. In LH-ALL, *TP53* 455
 456 mutation likely acts as the triggering event for genome instabil- 456
 457 ity, allowing the emergence of the low-hypodiploid clone respon- 457
 458 sible for leukemia onset. The further step of whole-genome 458
 459 duplication, whereas otherwise rare in ALL, may be also related 459
 460 to *TP53* deficiency, as reported in other tumors (35). 460

461 Moreover, we show that somatic *TP53* mutations in LH-ALL 461
 affect preleukemic HSPCs that retain their ability to gener-
 ate mature blood cells, defining clonal hematopoiesis. This

connects LH-ALL to the spectrum of hematologic malignancies related to *TP53*-mutant clonal hematopoiesis, namely, secondary and therapy-related AML and MDS having *TP53* biallelic alteration and complex karyotype (20–22). We also show that, at least in some cases, a myeloid premalignant clone may evolve concurrently to LH-ALL, which may support treatments aiming at eradicating not only B-ALL but *TP53*-mutant clonal hematopoiesis. Altogether, our study sheds light on an unsuspected link between LH-ALL, *TP53*-mutant clonal hematopoiesis, and related myeloid malignancies and paves the way for future investigations regarding its clinical and therapeutic relevance.

METHODS

Patients and Samples

The study cohort included patients with Ph-negative B-ALL ages 18 to 59 years enrolled in the GRAALL-2014 trial between 2016 and 2020 and French patients ages ≥ 55 years enrolled in the EWALL-INO trial between 2017 and 2022 (ClinicalTrials.gov number NCT02617004 and NCT03249870, respectively). The GRAALL-2014 protocol was an intensive pediatric-inspired treatment similar to the GRAALL-2005 (5), but with age adaptation of doses for patients 45 to 59 years old. The standard induction comprised prednisone, daunorubicin, vincristine, cyclophosphamide, L-asparaginase, and intrathecal prophylaxis. The EWALL-INO protocol was a treatment based on a low-intensity chemotherapy backbone and intrathecal prophylaxis with the addition of inotuzumab ozogamicin (INO) during the two-phase induction. The first induction phase comprised 3 doses of INO (D1: 0.8 mg/m², D8 and D15: 0.5 mg/m²) in combination with weekly vincristine 2 mg i.v. and dexamethasone 40 mg for 4 weeks, and the second phase comprised 2 doses of INO at 0.5 mg/m² in combination with dexamethasone 20 mg (D1 and D8) and cyclophosphamide 300 mg/m²/day i.v. D1–3. All the patients provided written informed consent for sample banking and analyses. The study was in accordance with the Declaration of Helsinki. Cytogenetic analyses at diagnosis were performed by local laboratories using standard procedures. Molecular analyses were performed centrally as previously described (36). Briefly, mononuclear cells from pretreatment bone marrow or peripheral blood samples were isolated by Ficoll centrifugation, and blast percentage was assessed by flow cytometry in most cases before nucleic acid extraction. MRD was assessed by the quantification of clonal *IG/TR* rearrangements, according to the EuroMRD guidelines.

Targeted DNA Sequencing

A custom panel of genes previously known to be targeted by recurrent mutations or CNA in B-ALL was analyzed by pan-exon capture-based target enrichment (SureSelectXT Low Input Target Enrichment System, Agilent) followed by library sequencing on the Illumina NextSeq500 platform (Illumina) as previously described (gene list in Supplementary Table S7; ref. 36). Data were analyzed for variant calling using Varscan (37) and Pindel (38), and CNA analysis was conducted using Viscap (39) and Facets (40). Lollipop plots were drawn with ProteinPaint (41).

B-ALL Classification Based on Cytogenetic and Molecular Data

B-ALL cases were first classified by the modal chromosome number of leukemia cells into three categories (≤ 40 , 41–49, and ≥ 50 chromosomes), referring to the major abnormal clone at karyotype analysis when it was informative (i.e., presence of abnormal mitosis) and DNA sequencing-based CNA analysis. Cases with ≤ 40 or ≥ 50 chromosomes were further examined as possibly being LH-ALL. By definition, all cases with 32 to 39 chromosomes (corresponding to 7–14 chromosome losses) were considered LH-ALL. Two additional cases having 40 chromosomes with a similar pattern of 7 chromosome losses and trisomy 21 were considered LH-ALL. Near haploidy was defined as 24 to 31 chromosomes. Within

cases with ≥ 50 chromosomes, LOH analysis allowed us to identify duplicated LH-ALL cases as cases with LOH affecting at 7 to 14 chromosomes. One case with LOH affecting 20 chromosomes was considered as duplicated near haploidy. High hyperdiploidy was defined as 51 to 65 chromosomes in the absence of other subtype-defining alteration.

TP53 Mutation Quantitation by Digital Droplet PCR

We performed ddPCR using the QX200 Droplet Digital PCR System (Bio-Rad) to track *TP53* mutations detected in bulk sequencing of diagnosis samples, in serial bone marrow posttreatment remission samples. Commercial assays for *TP53* p.R175H (dHsaMDV2010105), p.H214R (dHsaMDS2510824), and p.R248Q (dHsaMDV2010127) were used on the QX200 Droplet Digital PCR System (Bio-Rad). Reaction mix was prepared using 2 \times ddPCR TM Supermix for Probes (no dUTP), primers and probe mix (20 \times), restriction enzyme MseI 2U and 100 ng of genomic DNA as a template for ddPCR assay in a 96-well plate according to the manufacturer's protocol. Patients' diagnosis DNAs were used as positive control, peripheral blood mononuclear cells from healthy donors were used as negative control, and water was used instead of DNA for the nontemplate control reaction. Data were analyzed using QX Manager Software Standard edition, version 1.2 (Bio-Rad).

Combined Single-Cell Immunophenotyping and Genotyping

A custom scDNAseq panel was designed to cover relevant somatic mutations and common SNPs allowing the detection of LOH (Supplementary Table S8). Additional primers for amplicons of clone-specific *IG/TR* rearrangements were also included (Supplementary Table S9). Frozen bone marrow mononuclear cells were thawed, stained using the ADT panel TotalSeq-D Human Heme Oncology Cocktail, V1.0 (BioLegend; antibody list in Supplementary Table S10), and loaded into the Tapestry single-cell DNA genotyping platform (Mission Bio) to perform microfluidic encapsulation, lysis, and barcoding according to the manufacturer's protocol (Chemistry V2, PN_3360A). To improve erythroid cells identification, TotalSeq-D0574 anti-human CD235a (Glycophorin A) Antibody (BioLegend) was spiked at 1 μ g during the resuspension procedure (available only for EL_046 diagnostic sample). DNA and ADT libraries were prepared and underwent 2 \times 150 bp paired-end sequencing on a NextSeq 500 platform (Illumina).

Bioinformatics Analysis

Raw data were processed using Mission Bio's Tapestry Pipeline (DNA pipeline version 2.0.2 and Protein pipeline version 2.0.1) for preprocessing, alignment (reference genome hg19), cell barcode correction, cell identification, variant calling of DNA amplicons, and ADT-seq reads counting. Multiomics h5 files were then analyzed on R version 4.1.2 (R Foundation for Statistical Computing). TapestryR package was used to annotate variants: a genotype was considered informative if the single-cell sequencing depth was ≥ 5 reads. Variants were categorized as wild-type (WT) if VAF $< 10\%$, heterozygous (het) if VAF comprised between 10% and 90%, and homozygous (hom) if VAF $\geq 90\%$. Variants covered by < 5 reads were considered noninformative and labeled as "missing genotype." No genotype filtering was performed before integration with ADT-seq data, in order to avoid data attrition, as all genotypes (i.e., WT, heterozygous and hemizygous/homozygous mutations) are expected. The rate of the allelic dropout was evaluated based on heterozygous SNPs. False homozygous genotypes related to allelic dropout were observed in 1% to 18% of cells (Supplementary Fig. S7). Patient-specific amplicons targeting clone-specific *IG/TR* rearrangements were considered informative if detected in the diagnostic sample. The *IG/TR* amplicons were considered positive if covered by ≥ 5 reads.

ADT read counts and cell barcodes were extracted from h5 files and were analyzed using Seurat package V4.1.0 (42). Remission samples were merged before proceeding to protein expression analysis as similar cell compositions were expected. Diagnostic samples were analyzed separately. Cells with total ADT-seq read counts $\geq 100k$ were excluded

584 to minimize the presence of doublet cells in further analyses (Supple-
585 mentary Table S11). Centered log-ratio transformation was performed
586 to normalize reads across cells before scaling, and then principal compo-
587 nent analysis was performed on the normalized and scaled data. Dimen-
588 sional reduction of protein expression data was performed using UMAP
589 embedding and K-nearest neighbors and Louvain clustering algorithms
590 to identify cell populations based on ADT sequencing before undergoing
591 manual cell population labeling based on cell-surface marker expression.
592 Genotype data were then merged, and relative mutated proportions were
593 calculated for each cluster having at least 10 cells for interpretation.

594 FACS of Cell Populations

595 As a cross-validation experiment, diagnostic samples from two
596 patients were subjected to FACS in order to characterize genetic
597 alterations in distinct cell populations. Briefly, frozen cells were
598 thawed, stained with lineage-specific antibodies, and sorted on FAC-
599 SARIA III (BD Biosciences). Cell fractions underwent DNA extraction
600 using QIAamp DNA Microkit (Qiagen) followed by targeted sequenc-
601 ing for somatic mutations and ddPCR quantitation for *IG/TR*
602 clonal rearrangements.

603 Data Availability

604 Single-cell and bulk targeted sequencing data are accessible through
605 the EGA database (<https://www.ega-archive.org>) under accession num-
606 bers EGAS000011006784 and EGAS000011006901, respectively. Other
607 data are available upon reasonable request to the principal investigator.

608 Authors' Disclosures

609 S. Gachet reports grants from Fondation de France during the con-
610 duct of the study. V. Asnafi reports personal fees from Servier outside
611 the submitted work. L. Ades reports grants and personal fees from BMS,
612 personal fees from Novartis, AbbVie, and JAZZ pharma outside the sub-
613 mitted work. Y. Chalandon reports other support from MSD, Novartis,
614 Incyte, BMS, Pfizer, AbbVie, Roche, Jazz, Gilead, Amgen, Astra-Zeneca,
615 Servier, MSD, Roche, Gilead, Amgen, Incyte, AbbVie, Janssen, Jazz, and
616 Astra-Zeneca outside the submitted work. F. Huguet reports personal
617 fees from Novartis, Incyte, Amgen, Pfizer, and Servier outside the sub-
618 mitted work. No disclosures were reported by the other authors.

619 Authors' Contributions

620 **R. Kim:** Conceptualization, formal analysis, investigation, writing-
621 original draft, writing-review and editing. **H. Bergugnat:** Data
622 curation, investigation. **L. Larcher:** Data curation, investiga-
623 tion. **M. Duchmann:** Methodology, writing-review and edit-
624 ing. **M. Passet:** Data curation, investigation, writing-review and
625 editing. **S. Gachet:** Methodology. **W. Cuccuini:** Data curation.
626 **M. Lafage-Pochitaloff:** Data curation, writing-review and editing.
627 **C. Pastoret:** Resources. **N. Gardel:** Resources. **V. Asnafi:** Resources.
628 **B.W. Schafer:** Resources. **E. Delabesse:** Resources. **R. Itzykson:**
629 Resources. **L. Adès:** Resources. **Y. Hicheri:** Resources. **Y. Chalandon:**
630 Resources. **C. Graux:** Resources. **P. Chevallier:** Resources.
631 **M. Hunault:** Resources. **T. Leguay:** Resources. **F. Huguet:** Resources.
632 **V. Lhéritier:** Data curation, project administration. **H. Dombret:**
633 Project administration. **J. Soulier:** Supervision, writing-review and
634 editing. **P. Rousselot:** Project administration. **N. Boissel:** Project
635 administration. **E. Clappier:** Conceptualization, supervision, fund-
636 ing acquisition, writing-original draft, writing-review and editing.

637 Acknowledgments

638 R. Kim was a recipient of a PhD grant with financial support from
639 ITMO Cancer of Aviesan on funds administered by INSERM. The
640 study was supported by a grant from Force Hémato (2020). The
641 authors thank the patients and all the GRAALL investigators, phys-
642 ians, and biologists who contributed samples and data for this study.
643 The authors thank the Saint-Louis Molecular Hematology lab for

technical support, especially Hélène Boyer, Emilie Gaudas, Léna Yousfi, 644
and Océanne Richard. The authors also thank Stéphanie Mathis, Pierre 645
Lemaire, and Clémentine Chauvel for the flow cytometry evaluation of 646
ALL diagnostic samples. This work benefited from the genomic plat- 647
form facility of Institut de Recherche Saint-Louis (IRSL), supported 648
by Association Saint-Louis. This work was supported by THEMA, the 649
national center for precision medicine in leukemia. 650

The publication costs of this article were defrayed in part by the 651
payment of publication fees. Therefore, and solely to indicate this 652
fact, this article is hereby marked "advertisement" in accordance with 653
18 USC section 1734. 654

Note

Supplementary data for this article are available at Blood Cancer 656
Discovery Online (<https://bloodcancerdiscov.aacrjournals.org/>). 657

Received September 21, 2022; revised November 29, 2022; accepted 658
January 10, 2023; published first January 10, 2023. 659

REFERENCES

1. Sive JI, Buck G, Fielding A, Lazarus HM, Litzow MR, Luger S, et al. 661
Outcomes in older adults with acute lymphoblastic leukaemia (ALL): 662
results from the international MRC UKALL XII/ECOG2993 trial. *Br* 663
J Haematol 2012;157:463–71. 664
2. Hunault-Berger M, Leguay T, Huguet F, Leprêtre S, Deconinck E, 665
Ojeda-Urbe M, et al. A phase 2 study of L-asparaginase encapsulated 666
in erythrocytes in elderly patients with Philadelphia chromosome 667
negative acute lymphoblastic leukemia: The GRASPALL/GRAALL- 668
SA2-2008 study. *Am J Hematol* 2015;90:811–8. 669
3. Gökbuğten N, Dombret H, Ribera J-M, Fielding AK, Advani A, 670
Bassan R, et al. International reference analysis of outcomes in adults 671
with B-precursor Ph-negative relapsed/refractory acute lymphoblas- 672
tic leukemia. *Haematologica* 2016;101:1524–33. 673
4. Huguet F, Leguay T, Raffoux E, Thomas X, Beldjord K, Delabesse E, 674
et al. Pediatric-inspired therapy in adults with Philadelphia chro- 675
mosome-negative acute lymphoblastic leukemia: the GRAALL-2003 676
study. *J Clin Oncol* 2009;27:911–8. 677
5. Huguet F, Chevret S, Leguay T, Thomas X, Boissel N, Escoffre-Barbe M, 678
et al. Intensified therapy of acute lymphoblastic leukemia in adults: 679
report of the randomized GRAALL-2005 clinical trial. *J Clin Oncol* 680
2018;36:2514–23. 681
6. Chiaretti S, Vitale A, Cazzaniga G, Orlando SM, Silvestri D, Fazi P, 682
et al. Clinico-biological features of 5202 patients with acute lympho- 683
blastic leukemia enrolled in the Italian AIEOP and GIMEMA proto- 684
cols and stratified in age cohorts. *Haematologica* 2013;98:1702–10. 685
7. Roberts KG, Gu Z, Payne-Turner D, McCastlain K, Harvey RC, 686
Chen I-M, et al. High frequency and poor outcome of Philadelphia 687
chromosome-like acute lymphoblastic leukemia in adults. *J Clin* 688
Oncol 2017;35:394–401. 689
8. Lafage-Pochitaloff M, Baranger L, Hunault M, Cuccuini W, Lefebvre C, 690
Bidet A, et al. Impact of cytogenetic abnormalities in adults with 691
Ph-negative B-cell precursor acute lymphoblastic leukemia. *Blood* 692
2017;130:1832–44. 693
9. Creasey T, Barretta E, Ryan SL, Butler E, Kirkwood AA, 694
Leongamornlert D, et al. Genetic and genomic analysis of acute 695
lymphoblastic leukemia in older adults reveals a distinct profile 696
of abnormalities: analysis of 210 patients from the UKALL14 and 697
UKALL60+ clinical trials. *Haematologica* 2022;107:2051–63. 698
10. Harrison CJ, Moorman AV, Broadfield ZJ, Cheung KL, Harris RL, 699
Reza Jalali G, et al. Three distinct subgroups of hypodiploidy in acute 700
lymphoblastic leukaemia. *Br J Haematol* 2004;125:552–9. 701
11. Charrin C, Thomas X, Ffrench M, Le Q-H, Andrieux J, Mozziconacci M-J, 702
et al. A report from the LALA-94 and LALA-SA groups on hypo- 703
diploidy with 30 to 39 chromosomes and near-triploidy: 2 possible 704
expressions of a sole entity conferring poor prognosis in adult acute 705
lymphoblastic leukemia (ALL). *Blood* 2004;104:2444–51. 706

- 707 12. Nachman JB, Heerema NA, Sather H, Camitta B, Forestier E, 759
 708 Harrison CJ, et al. Outcome of treatment in children with hypodip- 760
 709 loid acute lymphoblastic leukemia. *Blood* 2007;110:1112-5. 761
- 710 13. Holmfeldt L, Wei L, Diaz-Flores E, Walsh M, Zhang J, Ding L, et al. 762
 711 The genomic landscape of hypodiploid acute lymphoblastic leuke- 763
 712 mia. *Nat Genet* 2013;45:242-52. 764
- 713 14. Mühlbacher V, Zenger M, Schnittger S, Weissmann S, Kunze F, 765
 714 Kohlmann A, et al. Acute lymphoblastic leukemia with low hypodip- 766
 715 loid/near triploid karyotype is a specific clinical entity and exhibits 767
 716 a very high TP53 mutation frequency of 93%. *Genes Chromosomes 768*
 717 *Cancer* 2014;53:524-36. 769
- 718 15. Stengel A, Schnittger S, Weissmann S, Kuznia S, Kern W, Kohlmann A, 770
 719 et al. TP53 mutations occur in 15.7% of ALL and are associated with 771
 720 MYC-rearrangement, low hypodiploidy, and a poor prognosis. *Blood 772*
 721 2014;124:251-8. 773
- 722 16. Kanagal-Shamanna R, Jain P, Takahashi K, Short NJ, Tang G, Issa GC, 774
 723 et al. TP53 mutation does not confer a poor outcome in adult patients 775
 724 with acute lymphoblastic leukemia who are treated with frontline 776
 725 hyper-CVAD-based regimens. *Cancer* 2017;123:3717-24. 777
- 726 17. Jaiswal S, Fontanillas P, Flannick J, Manning A, Grauman PV, Mar BG, 778
 727 et al. Age-related clonal hematopoiesis associated with adverse out- 779
 728 comes. *N Engl J Med* 2014;371:2488-98. 780
- 729 18. Genovese G, Köhler AK, Handsaker RE, Lindberg J, Rose SA, 781
 730 Bakhoum SF, et al. Clonal hematopoiesis and blood-cancer risk 782
 731 inferred from blood DNA sequence. *N Engl J Med* 2014;371:2477-87. 783
- 732 19. Xie M, Lu C, Wang J, McLellan MD, Johnson KJ, Wendl MC, et al. Age- 784
 733 related mutations associated with clonal hematopoietic expansion 785
 734 and malignancies. *Nat Med* 2014;20:1472-8. 786
- 735 20. Wong TN, Ramsingh G, Young AL, Miller CA, Touma W, Welch JS, 787
 736 et al. Role of TP53 mutations in the origin and evolution of therapy- 788
 737 related acute myeloid leukaemia. *Nature* 2015;518:552-5. 789
- 738 21. Gillis NK, Ball M, Zhang Q, Ma Z, Zhao Y, Yoder SJ, et al. Clonal 790
 739 haemopoiesis and therapy-related myeloid malignancies in elderly 791
 740 patients: a proof-of-concept, case-control study. *Lancet Oncol 792*
 741 2017;18:112-21. 793
- 742 22. Abelson S, Collord G, Ng SWK, Weissbrod O, Mendelson Cohen N, 794
 743 Niemeyer E, et al. Prediction of acute myeloid leukaemia risk in healthy 795
 744 individuals. *Nature* 2018;559:400-4. 796
- 745 23. Miles LA, Bowman RL, Merlinsky TR, Csete IS, Ooi AT, 797
 746 Durruthy-Durruthy R, et al. Single-cell mutation analysis of clonal 798
 747 evolution in myeloid malignancies. *Nature* 2020;587:477-82. 799
- 748 24. Morita K, Wang F, Jahn K, Hu T, Tanaka T, Sasaki Y, et al. Clonal 800
 749 evolution of acute myeloid leukemia revealed by high-throughput 801
 750 single-cell genomics. *Nat Commun* 2020;11:5327. 802
- 751 25. Demaree B, Delley CL, Vasudevan HN, Peretz CAC, Ruff D, Smith CC, 803
 752 et al. Joint profiling of DNA and proteins in single cells to dis- 804
 753 sect genotype-phenotype associations in leukemia. *Nat Commun 805*
 754 2021;12:1583. 806
- 755 26. Boettcher S, Miller PG, Sharma R, McConkey M, Leventhal M, 807
 756 Krivtsov AV, et al. A dominant-negative effect drives selection of 808
 757 TP53 missense mutations in myeloid malignancies. *Science* 2019;365: 809
 758 599-604. 810
27. Mullighan CG, Su X, Zhang J, Radtke I, Phillips LAA, Miller CB, et al. 759
 Deletion of IKZF1 and prognosis in acute lymphoblastic leukemia. *N 760*
Engl J Med 2009;360:470-80. 761
28. Mullighan CG, Zhang J, Kasper LH, Lerach S, Payne-Turner D, 762
 Phillips LA, et al. CREBBP mutations in relapsed acute lymphoblastic 763
 leukaemia. *Nature* 2011;471:235-9. 764
29. Zhao Y, Aldoss I, Qu C, Crawford JC, Gu Z, Allen EK, et al. Tumor- 765
 intrinsic and -extrinsic determinants of response to blinatumomab in 766
 adults with B-ALL. *Blood* 2021;137:471-84. 767
30. Mar BG, Bullinger LB, McLean KM, Grauman PV, Harris MH, 768
 Stevenson K, et al. Mutations in epigenetic regulators including 769
 SETD2 are gained during relapse in paediatric acute lymphoblastic 770
 leukaemia. *Nat Commun* 2014;5:3469. 771
31. Mar BG, Chu SH, Kahn JD, Krivtsov AV, Koche R, Castellano CA, 772
 et al. SETD2 alterations impair DNA damage recognition and lead to 773
 resistance to chemotherapy in leukemia. *Blood* 2017;130:2631-41. 774
32. Shlush LI, Zandi S, Mitchell A, Chen WC, Brandwein JM, Gupta V, 775
 et al. Identification of pre-leukaemic haematopoietic stem cells in 776
 acute leukaemia. *Nature* 2014;506:328-33. 777
33. Beer PA, Delhommeau F, LeCouédic J-P, Dawson MA, 778
 Chen E, Bareford D, et al. Two routes to leukemic transformation 779
 after a JAK2 mutation-positive myeloproliferative neoplasm. *Blood 780*
 2010;115:2891-900. 781
34. Hof J, Krentz S, van Schewick C, Körner G, Shalpour S, Rhein P, 782
 et al. Mutations and deletions of the TP53 gene predict nonresponse 783
 to treatment and poor outcome in first relapse of childhood acute 784
 lymphoblastic leukemia. *J Clin Oncol* 2011;29:3185-93. 785
35. Bielski CM, Zehir A, Penson AV, Donoghue MTA, Chatila W, 786
 Armenia J, et al. Genome doubling shapes the evolution and prognos- 787
 is of advanced cancers. *Nat Genet* 2018;50:1189-95. 788
36. Passet M, Boissel N, Sigaux F, Saillard C, Bargetzi M, Ba I, et al. PAX5 789
 P80R mutation identifies a novel subtype of B-cell precursor acute 790
 lymphoblastic leukemia with favorable outcome. *Blood* 2019;133:280-4. 791
37. Koboldt DC, Zhang Q, Larson DE, Shen D, McLellan MD, Lin L, et al. 792
 VarScan 2: somatic mutation and copy number alteration discovery 793
 in cancer by exome sequencing. *Genome Res* 2012;22:568-76. 794
38. Ye K, Schulz MH, Long Q, Apweiler R, Ning Z, Pindel: a pat- 795
 tern growth approach to detect break points of large deletions and 796
 medium sized insertions from paired-end short reads. *Bioinformatics 797*
 2009;25:2865-71. 798
39. Pugh TJ, Amr SS, Bowser MJ, Gowrisankar S, Hynes E, Mahanta LM, 799
 et al. VisCap: inference and visualization of germ-line copy-number vari- 800
 ants from targeted clinical sequencing data. *Genet Med* 2016;18:712-9. 801
40. Shen R, Seshan VE. FACETS: allele-specific copy number and clonal 802
 heterogeneity analysis tool for high-throughput DNA sequencing. 803
Nucleic Acids Res 2016;44:e131. 804
41. Zhou X, Edmonson MN, Wilkinson MR, Patel A, Wu G, Liu Y, et al. 805
 Exploring genomic alteration in pediatric cancer using ProteinPaint. 806
Nat Genet 2016;48:4-6. 807
42. Hao Y, Hao S, Andersen-Nissen E, Mauck WM, Zheng S, 808
 Butler A, et al. Integrated analysis of multimodal single-cell data. *Cell 809*
 2021;184:3573-87. 810